Optimization of an Environmentally Sustainable HTL-Free Perovskite Solar Cell using SCAPS-1D

Ola Mostafa[1], Hanady Hussein Issa[2], M. Fedawy[2,3], Wael Abbas[1], Nehad Zidan[4]

[1]Basic and Applied Sciences Department, College of Engineering and Technology, Arab Academy for Science and Technology, Cairo, Egypt.
[2]Electronics and Communications Engineering Department, College of Engineering and Technology, Arab Academy for Science and Technology, Cairo, Egypt.

[3]Center of Excellence in Nanotechnology, Arab Academy for Science and Technology and Maritime Transport, Cairo P.O. Box 2033, Egypt.

[4]Physics and Engineering Mathematics Department, Faculty of Engineering- Elmattaria, Helwan University, Cairo, Egypt.

Abstract

Perovskite solar cells (PSCs) without a hole transport layer (HTL) are proposed in this study as a more cost-effective and efficient alternative to PSCs with an HTL. The active layer of these cells is $CH_3NH_3SnI_3$. To optimize the performance of the proposed PSC, different materials for Electron Transport Layers (ETLs) were simulated. Additionally, the impact of thickness, doping concentration, and doping concentration profile on device performance was investigated using a 1D-Solar Cell Capacitance Simulator. According to the simulation results, the optimal thicknesses of the ETL and the absorber were 30 nm and 1000 nm respectively, resulting in a power conversion efficiency (PCE) of 31.08 %. The proposed HTL-free $CH_3NH_3SnI_3$.-based PSC attained an open circuit voltage of 1.1037 V, a short-circuit current density of 31.749 mA/cm^2, and a fill factor of 88.7 %. These results may help in the creation of highly effective and reasonably priced solar cells by providing insight into the design and optimization of HTL-free PSCs. Given that it provides a simple and inexpensive method of producing high-performance solar cells, the suggested PSC structure has the potential to be a viable replacement for traditional PSCs with HTL.

1. Introduction

With the growth of the global population, there has been a corresponding increase in energy consumption. However, using non-renewable energy sources like fossil fuels has contributed to environmental problems, prompting a greater focus on renewable energy. One particularly important renewable energy source is solar energy, which is abundant,

clean, and infinitely available [1]. Solar energy is an environmentally friendly energy source that has garnered significant attention in recent years due to its potential to meet the rising energy demand and prevent climate change. Using photovoltaic devices, such as solar cells, sunlight is converted into electrical energy [2]. Silicon-based solar cells have been the most extensively utilized form of solar cell due to their high efficiency and stability. Nevertheless, the expense of silicon solar cells continues to be a significant barrier to their widespread adoption [3]. Researchers have concentrated on creating alternative solar cell materials and architectures that may provide more efficiency, cheaper cost, and greater flexibility to overcome this problem. Perovskite solar cells (PSCs) are among the most optimal choices for this purpose [4-5]. Over the last decade, the power conversion efficiency (PCE) of PSCs increased dramatically from 3.13 % [6] to 25.8 % [7]. PSCs are manufactured at a cheap cost utilizing solution-based techniques such as spin-coating, inkjet printing, and spray-coating. PSCs are, therefore very scalable and ideal for large-scale manufacture. Perovskite materials have several benefits, including an adaptable bandgap and a high absorption coefficient [8]. Despite their promising potential, PSCs encounter a number of obstacles that must be investigated in order to optimize their performance. The use of toxic and costly materials, such as lead, in the perovskite layer is one of the challenges [9]. To address this issue, researchers have concentrated on developing lead-free perovskite materials with comparable effectiveness and less harmful effects on the environment [10-11]. A solar cell's basic structure consists of a narrow layer of semiconductor material sandwiched between two electrode layers. Typically, the upper electrode consists of a narrow layer of metal, such as aluminium, while the bottom electrode consists of a thicker layer of metal, such as copper. When sunlight impacts a semiconductor material, electron-hole pairs are created, which are then separated by the electric field produced by the p-n junction. The top electrode collects the electrons, which then travel through an external circuit to generate an electric current. Between the semiconductor layer and the bottom electrode lies a layer of material called the the electron transport layer (ETL). Its purpose is to move the negatively charged carriers (electrons), which are produced when sunlight hits the semiconductor material, to the bottom electrode. Contrarily, the hole transport layer (HTL) is a material layer sandwiched between the semiconductor layer and the top electrode. Its purpose is to move holes, the positively charged carriers produced when sunlight hits semiconductor material, to the top electrode [12]. HTLs are usually made of organic or inorganic materials that are often toxic or costly. This makes it hard to use them in large-scale production. A free HTL in lead-free PSCs has been indicated as an innovative technique to solve this problem. This technique reduces the need for an extra HTL material and lowers the cost of the solar cell. Also, using this

technique allows for more stability of the device, as well as making the process of fabricating the device simpler.

In this context, the purpose of this study is to examine the efficiency of using a free hole transport layer in lead-free PSCs. The study will concentrate on optimizing the structure of the device and characterizing its performance, including its PCE, fill factor (FF), open-circuit voltage (V_{oc},), and short-circuit current density (J_{sc}). To accomplish this, various materials for Electron Transport Layers (ETLs) will be emulated, and the impact of thickness, doping concentration, and doping concentration profile will be investigated using a 1D-Solar Cell Capacitance Simulator, with all simulations conducted under AM1.5G at a temperature of 300 K. The optimization approach will involve using an initial structure that utilizes TiO_2 as the ETL and Spiro-MeOTAD as the HTL, based on prior experimental work [13]. Overall, the goal of this research is to investigate the possibility of using a free hole transport layer in lead-free PSCs solar cells and to optimize the device's structure to achieve superior performance.

2. Structure and material parameters of the device

SCAPS-1D is a program created by the University of Gent in Belgium that is commonly utilized for modeling the electrical properties of solar cells. SCAPS-1D simulates the performance of a solar cell by considering numerous physical characteristics and material properties such as layer thickness, doping concentration, and charge carrier mobility. The SCAPS program can compute the performance parameters of solar cells by using the numerical solutions of the fundamental semiconductor equations [14]. These equations include the electron (1) and hole (2) continuity equations as well as the Poisson Eq. (3). These equations are presented below:

$$\nabla . J_n = q(R - G) + q\frac{\partial n}{\partial t} \quad (1)$$

$$-\nabla . J_p = q(R - G) + q\frac{\partial p}{\partial t} \quad (2)$$

$$\nabla . \varepsilon \nabla \varphi = -\mathrm{q}(\mathrm{p} - \mathrm{n} + N_D - N_A) \quad (3)$$

In order to determine the necessary properties of the solar cells, the equations mentioned previously are solved numerically with SCAPS-1D software by adjusting the material parameters and appropriate boundary conditions. In this equation, N_A and N_D represent the acceptor and donor doping concentrations, φ is the electric potential, p and n are the free carrier hole and electron concentrations, J_n and J_p are the electron current density and hole current density, and R and G are the recombination and generation rates of electron-hole pairs. The experimental structure shown in Figure 1 was calibrated using a SCAPS-1D.

Each layer in this multi-layered structure is essential to transferring charge carriers and converting sunlight into energy.

Table 1. Simulation physical parameters (CB = conduction band, VB = valence band, DOS = density of states) [15].

Parameters	TCO	TiO_2	$CH_3NH_3SnI_3$	Spiro-OmeTAD
Thickness (nm)	500	30	350	200
Bandgap (eV)	3.5	3.2	1.3	3.17
Electron affinity χ (eV)	4	4.26	4.17	2.05
Relative Dielectric permittivity (ε_r)	9	9	8.2	3
CB effective DOS (cm^{-3})	2.2×10^{18}	2×10^{18}	1×10^{18}	2.2×10^{18}
VB effective DOS (cm^{-3})	1.8×10^{19}	1.8×10^{19}	1×10^{18}	1.8×10^{19}
Electron mobility μ_n ($cm^2/V.\ s$)	20	20	1.6	2×10^{-4}
Hole mobility μ_p ($cm^2/V.\ s$)	10	10	1.6	2×10^{-4}
Donor concentration N_D (cm^{-3})	2×10^{19}	1×10^{16}	0	0
Acceptor concentration N_A (cm^{-3})	0	0	3.2×10^{15}	2×10^{19}
Defect density N_t (cm^{-3})	1×10^{15}	1×10^{15}	10^{16}-10^{15}	1×10^{15}
Thermal velocities V_{tht} (cm/s)	1×10^{7}	1×10^{7}	1×10^{7}	1×10^{7}

The glass basis is used as a support for the whole solar cell structure, starting at the lowest layer. The Transparent Conductive Oxide (TCO) layer, which acts as a front electrode and helps in the collection of electrons from the absorption layer, is placed next. After that, ETL is responsible for facilitating the movement of electrons from the absorption layer to the front electrode. Solar energy is turned into electrical energy in the perovskite absorption layer. HTL is placed on top of the absorption layer and facilitates the movement of holes from the absorption layer to the back electrode. Finally, the back electrode serves as the other contact for the solar cell and helps in the collection of holes. The thermal velocities

of the electrons and holes in this simulation were both set to 10^7 cm/s. The capture cross-section for both electrons and holes were adjusted at 1×10^{-15} cm^2, and the defect type in all layers was neutral.

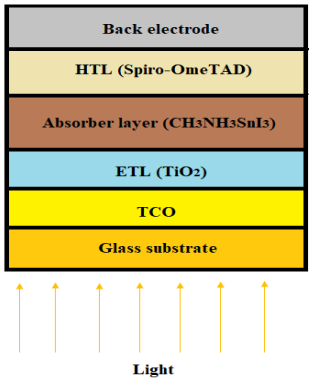

Figure 1 Basic lead-free PSCs structure

3. Device Model Verification

Our simulation results were calibrated with the experimental data [13]. Table 1 shows each layer's simulation parameters [15]. The calibrated structure consists of a glass substrate, a Transparent Conductive Oxide (TCO) layer, an ETL of TiO_2 , a $CH_3NH_3SnI_3$. absorption layer, and a spiro-OMeTAD HTL with a metal back contact. Figure 2 depicts the J-V curve for the basic lead-free PSCs structure with various N_t (trap density) values. Our simulation's results were well-aligned with experimental measurements, as indicated in Table 2. As shown in Figure 2, when N_t increases, the J-V curves shift towards lower current values, indicating a decrease in the efficiency of the solar cell. To enhance the efficacy of the cell, the initial defect density N_t must be decreased in order to increase the diffusion length and reduce the recombination rate. Practically it is extremely difficult to set N_t below 1×10^{15}.

Table 2. Comparison of Experimental and Simulated Results.

lead-free PSC	V_{oc} (V)	J_{sc} (mA/cm^2)	FF (%)	PCE (%)
Experimental [12]	0.68±0.03	16.30±0.71	48±3	5.23±0.18
Simulated (N_t=5*$10^{17}/cm^3$)	0.6767	17.450194	45.98	5.43

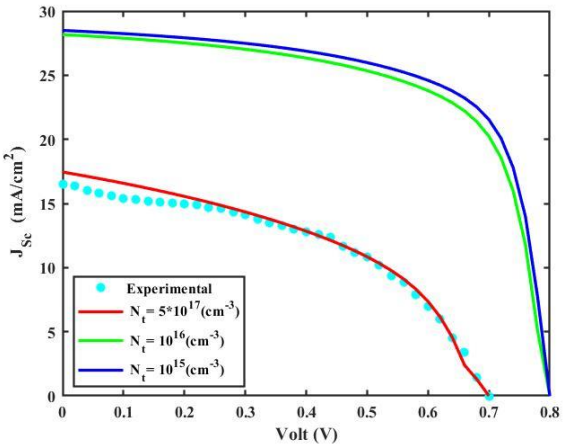

Figure 2 J-V curves for basic structures with varying N_t compared to experimental data.

4. Results and discussion

In this part, the proposed structure of lead-free PSC that is HTL-free was studied. Electron Transport Materials (ETMs) were investigated, followed by an optimization process to determine the optimal thickness and doping concentrations for both the ETL and the absorption layer.

4.1 HTL-Free Structure for Lead-Free PSC

The HTL-free structure for lead-free PSC typically consists of TCO layer, ETL, a perovskite absorber layer, a metal electrode, and a substrate, as shown in Figure 3. The TCO layer serves as the bottom electrode. Its primary function is to allow light to pass through to the perovskite absorber layer while simultaneously conducting electricity. The ETL must be able to efficiently extract electrons from the perovskite absorber layer and transport them to the back electrode. The perovskite absorber layer, which is the device's active layer, absorbs sunlight and generates charges. Finally, the metal electrode collects the electrons generated by the perovskite absorber layer and transports them out of the device. The proposed HTL-free structure offers several benefits over traditional PSC designs. Firstly, it simplifies the device structure, reducing production costs and simplifying manufacturing processes. Secondly, it eliminates the need for HTL materials, which are often unstable and can contribute to device degradation over time. Thirdly, the HTL-free structure can improve charge extraction efficiency from the perovskite absorber layer [16]. In traditional PSC designs, the HTL layer can impede the transport of holes, leading to decreased device efficiency. By eliminating the HTL layer, the charge extraction process can become more efficient, increasing overall device efficiency.

The performance of lead-free PSC without a hole transport layer can be enhanced by decreasing the trap density, as traps can act as charge carrier recombination centers, therefore reducing the solar cell's efficiency, as indicated in Table 3. By decreasing the trap density, there are fewer chances for charge carriers to recombine, which can increase the solar cell's overall efficiency. In addition, removing the hole transport layer can reduce the number of interfaces in the device, which reduces recombination and enhances the solar cell's performance.

Table 3. Simulation Results for lead-free PSC without HTL

$N_t\ (/cm^3)$	V_{oc} (V)	$J_{Sc}\ (mA/cm^2)$	FF (%)	PCE (%)
$5*10^{17}$	0.6837	18.207214	49.55	6.17
$1*10^{16}$	0.7945	28.471366	70.57	15.96

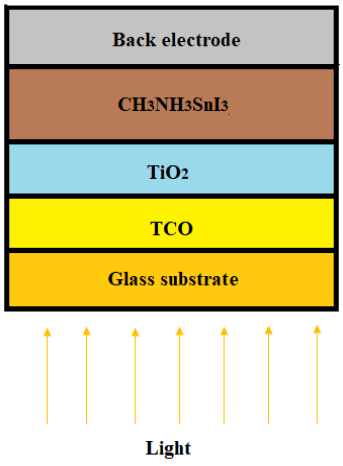

Figure 3 HTL-free structure for lead-free PSC.

4.2 Optimizing ETL

In this section, we optimize the ETL by exploring different materials to determine the most suitable Electron Transport Material (ETM) and the optimal thickness and doping concentration. Table 4 presents the input parameters for the various ETMs considered. In contrast, the energy band diagrams of the materials studied in this work are shown in Figure 4. Table 5 summarizes the device's performance for the different ETMs considered.

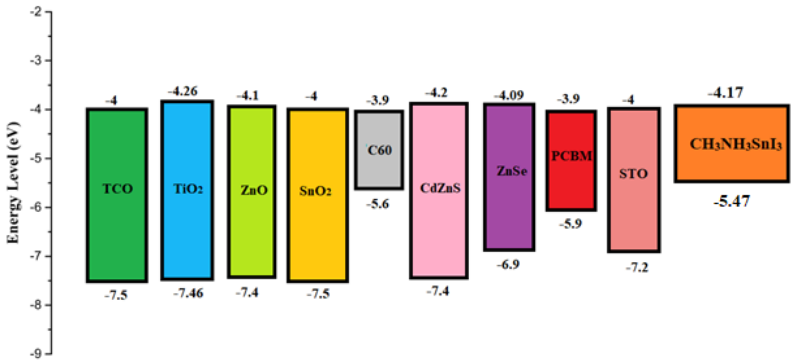

Figure 4 ETM energy band diagrams

Table 4. Input Parameters various ETMs.

Parameters	ZNO [17]	PCBM [17]	SnO_2 [18]	CdZnS [17]	Ws_2 [17]	STO [19]	ZnSe [19]	C60 [17]
Thickness (nm)	30	30	30	30	30	30	30	30
Bandgap (eV)	3.3	2	3.5	3.2	1.8	3.2	2.81	1.7
Electron affinity χ (eV)	4.1	3.9	4	4.2	3.95	4	4.09	3.9
Relative Dielectric permittivity (ε_r)	9	3.9	9	9.120	13.6	8.7	8.6	4.2
CB effective DOS (cm^{-3})	4×10^{18}	2.5×10^{21}	2.2×10^{17}	1.5×10^{18}	2.2×10^{18}	1.7×10^{19}	2.2×10^{18}	8×10^{19}
VB effective DOS (cm^{-3})	1×10^{19}	2.5×10^{21}	2.2×10^{16}	1.8×10^{19}	1.9×10^{19}	2×10^{20}	1.8×10^{18}	8×10^{19}
Electron mobility μ_n ($cm^2/V.s$)	1×10^{2}	2×10^{-1}	2×10^{1}	2.5×10^{2}	1×10^{2}	5.3×10^{3}	4×10^{2}	8×10^{-2}
Hole mobility μ_p ($cm^2/V.s$)	2.5×10^{1}	2×10^{-1}	1×10^{1}	4×10^{1}	1×10^{2}	6.6×10^{2}	1×10^{-1}	3.5×10^{-3}

Based on the simulation findings, SnO_2 has been shown to be the most effective ETL material in the proposed device resulting in an efficiency of 18.66 %, as is seen in Table 5. It is likely the reason because SnO_2 has a large work function, which makes charge extraction easier and reduces recombination losses at the perovskite/ETL interface. Additionally, the energy level alignment between SnO_2 and the perovskite layer is favorable, which allows for efficient charge transfer across the interface. These properties of SnO_2 make it suitable for use as an ETL in lead-free lead-free PSC without an HTL, leading to the highest performance among the ETMs considered in the study.

Table 5. The device's performance for serval ETMs

Material	PCE (%)	FF (%)	J_{Sc} (mA/cm^2)	V_{oc} (V)
TiO_2	15.96%	70.57	28.4713	0.7945
ZNO	17.87%	72.44	28.7736	0.8571
PCBM	16.50%	71.74	27.0467	0.8504
SnO_2	**18.66%**	**74.27**	**29.1062**	**0.8633**
CdZnS	17.10%	71.1	28.6269	0.84
Ws_2	17.23%	74.56	26.8459	0.861
STO	18.25%	73.4	28.8762	0.861
ZnSe	17.91%	72.83	28.6388	0.8588
C60	14.73%	69.48	25.751	0.8235

4.3The Effects of Varying ETL Thickness on the device Performance

This Section focuses on the optimization of ETL thickness in the proposed device. In this work, we investigate the effects of varying ETL thickness on device performance, ranging from 10 nm to 500 nm, and find that as the thickness of the ETL decreases, the solar cell's performance tends to improve, as clearly from Figure 5. However, there is a lower limit to how thin the ETL can be made due to manufacturing issues. In particular, ETL thickness of less than 30 nm is difficult to achieve with current manufacturing techniques. This is because very thin ETL layers are more prone to defects and inconsistencies, which can negatively impact device performance. Therefore, decreasing ETL thickness can lead to improved performance for several reasons. First, a thinner ETL reduces the distance that electrons have to travel to reach the electrode, which can improve charge extraction efficiency and reduce losses due to recombination. Second, a thinner ETL can reduce

the energy barrier at the interface between the perovskite layer and the electrode, allowing for more efficient charge transfer and reducing losses due to charge trapping or recombination [19]. The proposed device considered an ETL thickness of 30 nm, resulting in a PCE of 18.66% with FF of 74.27%, J_{sc} of 29.106 mA/cm^2 and V_{oc} of 0.8633 V.

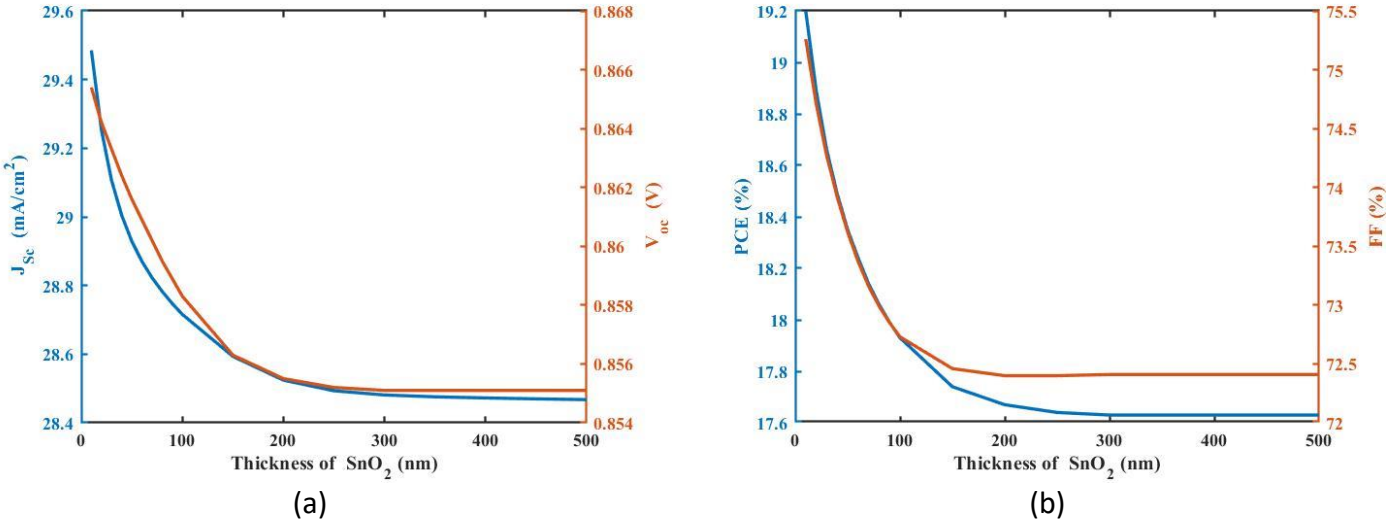

Figure 5 The device's performance for serval SnO_2 thickness (a) J-V, (b) PCE-FF

4.3.1 The Effects of ETL doping concentration on the device performance

In this section, the effect of ETL doping concentration in lead-free perovskite solar cells that do not include HTL is studied. The doping concentration is varied from $N_D = 10^{16}$ to 10^{21} cm^{-3} . The performance of the proposed device is strongly influenced by the doping concentration of the ETL. The optimal doping concentration is found to be $N_D = 10^{21}$ cm^{-3}, which leads to the highest PCE of 20.05%. This increase in efficiency is primarily attributed to the improved conductivity of the ETL material, which enhances the transfer of electrons from the perovskite layer to the electrode, reducing losses due to recombination. In addition, increasing the doping concentration also modifies the energy level alignment between the ETL and the perovskite layer, facilitating more efficient charge transfer across the interface. These combined effects result in higher open circuit voltage, short circuit current density, and overall power conversion efficiency, as illustrated in Figure 6.

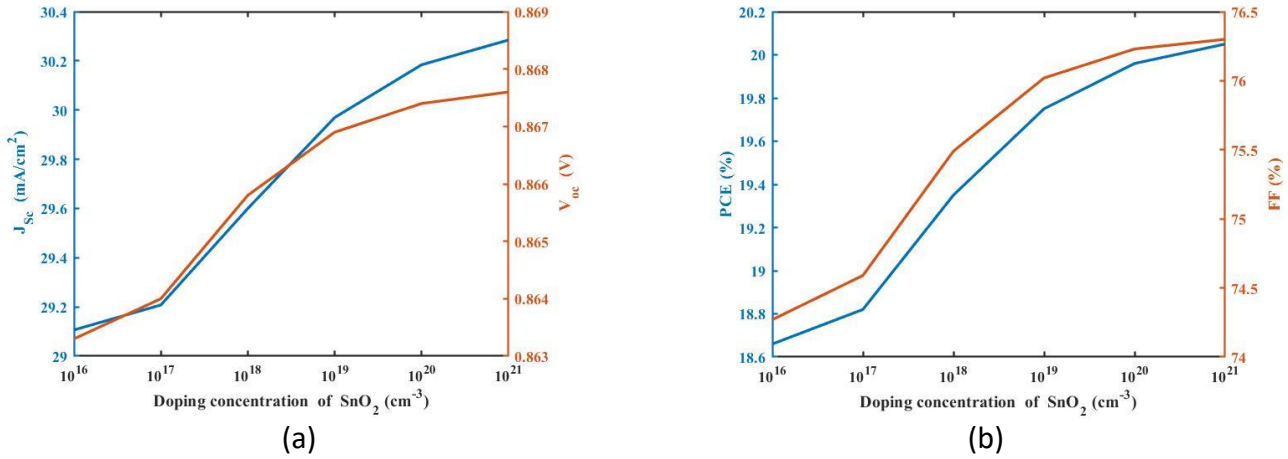

Figure 6 The device's performance for variation of SnO_2 doping (a) J-V, (b) PCE-FF

4.4 Optimizing lead-free perovskite layer

The perovskite layer is a critical layer in the achievement of high-performance solar cells. In this paper, we focus specifically on optimizing the lead-free perovskite layer ($CH_3NH_3SnI_3$) by determining the optimal thickness and doping concentration, while keeping the defect type neutral with value of $1*10^{16}/cm^3$.

4.4.1 The Effects of Varying the perovskite layer Thickness on the device Performance

In this section, the optimal thickness of the perovskite layer ($CH_3NH_3SnI_3$) in the proposed lead-free PSC without HTL is investigated. We examine the impact of varying the perovskite layer thickness within the range of 100 nm to 1300 nm on the proposed device's performance. Our results reveal that as the thickness of the perovskite layer increases, the performance of the solar cell generally improves, as evidenced by the data presented in Figure 7. Specifically, we find that the optimal thickness for the perovskite layer is at 1000 nm, resulting in PCE of 21.56 % with FF of 74.4 %, J_{sc} of 33.11mA/cm^2 and V_{oc} of 0.8752 V, beyond which the performance of the solar cell becomes saturated. The reason for that is that a thicker perovskite layer can absorb more light, generating a higher number of electron-hole pairs, which in turn increases the current output and thus the efficiency of the solar cell as shown in Figure 7.b. Additionally, the thicker perovskite layer reduces the probability of charge recombination, which can occur when the electron and hole pairs meet and neutralize each other before they can be collected as current [21]. This is because a thicker perovskite layer provides a greater distance for the charge carriers to

travel before they recombine, increasing the chances that they will be collected as current instead as illustrated in figure 7.a. This improved performance continues until a certain thickness is reached, beyond which the benefits of additional thickness become saturated, and the performance of the solar cell levels off or even decreases.

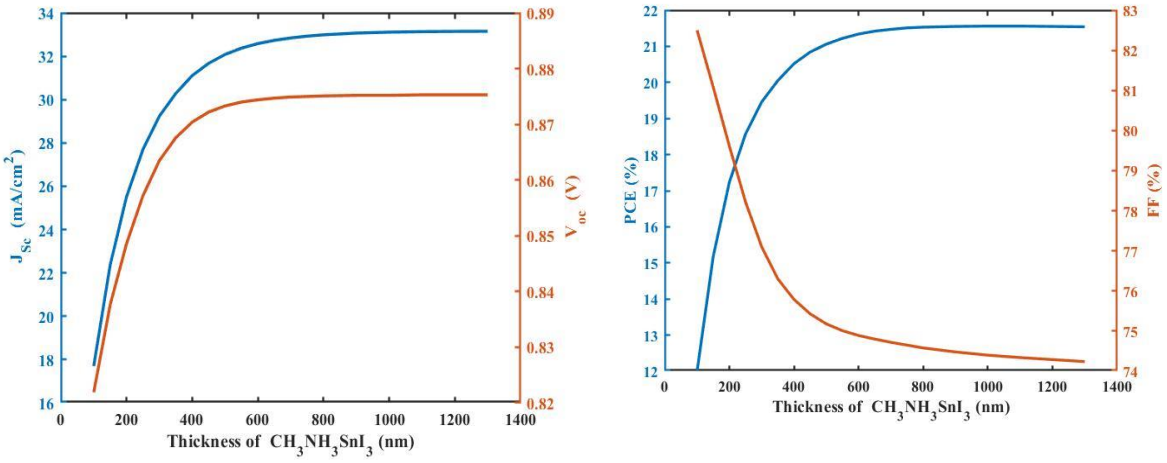

(a) (b)

Figure 7 The device's performance for serval perovskite layer thickness (a) J-V, (b) PCE-FF

4.4.2 The impact of the doping concentration of the perovskite layer on the performance of the proposed device.

This section focuses on studying the impact of the doping concentration of the perovskite layer on the performance of the lead-free perovskite solar cell without HTL. We investigate the effects of doping concentrations ranging from 10^{16} cm^{-3} to 10^{21} cm^{-3} and observe that the performance of the device generally improves as the doping concentration increases up to a specific value, after which it begins to decrease, as shown in Figure 8. Low doping concentrations limit the number of free charge carriers, leading to low current output and poor device performance. As the doping concentration increases, the number of free charge carriers also increases, leading to improved current output and higher efficiency. H While a doping concentration of 10^{16} cm^{-3} can result in a high PCE of 21.51%, it is essential to note that beyond this concentration, the recombination rate of the charge carriers may increase, leading to reduced efficiency and decreased device performance.

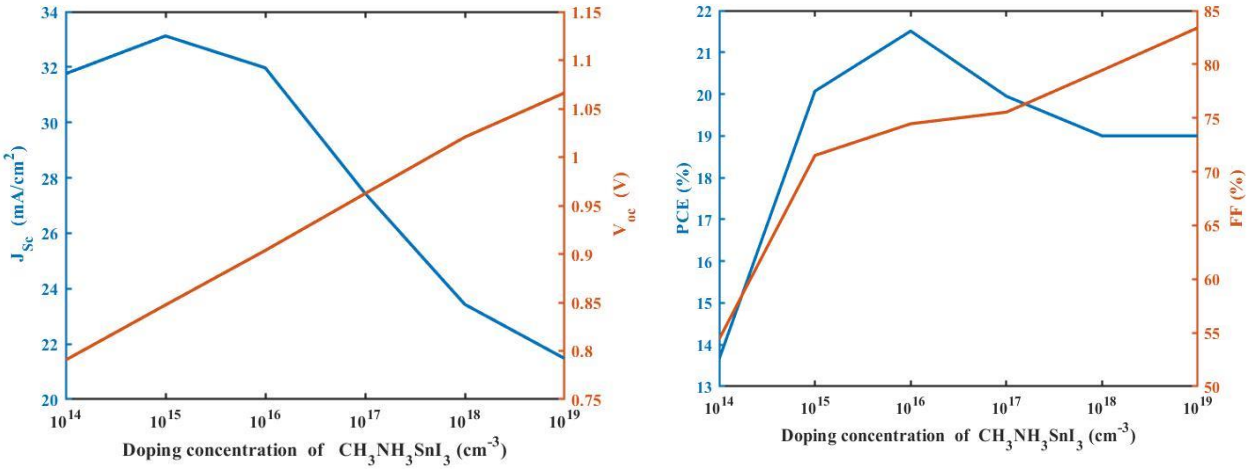

(a) (b)

Figure 8 The device's performance for variation of $CH_3NH_3SnI_3$ doping concentration

(a) J-V, (b) PCE-FF

4.4.3 The impact of the doping concentration profile of the perovskite layer on the performance of the proposed device.

In this section, we investigate the impact of the different doping concentration profile of the perovskite layer ($CH_3NH_3SnI_3$) on the performance of the proposed device. While the previous results focused on a uniform doping type, we change the doping concentration profile to a linear doping type to examine its effect on the device performance. The difference between the two doping profiles lies in the distribution of free charge carriers within the perovskite layer. In a uniform doping profile, the density of free charge carriers is the same at all locations within the layer, while in a linear doping profile, the density of free charge carriers varies across the layer. This can affect the transport of charge carriers within the perovskite layer, as well as their recombination rate and overall efficiency. Based on the data presented in Table 6, it appears that the linear doping profile enhances the performance of the proposed device more than the uniform doping profile. Furthermore, reducing the defect density from 10^{16} cm^{-3} to 10^{15} cm^{-3} and using a linear doping profile leads to the highest efficiency. The proposed structure has achieved an efficiency of up to 31.7%

Table 6. Comparison of Performance of Non-Toxic, HTL-Free PSC with Uniform and Linear Doping Profiles Under Different Defect Densities

Doping Profile	Defect Density (cm^{-3})	V_{oc} (V)	J_{Sc} (mA/cm^2)	FF (%)	PCE (%)
Uniform	10^{16}	0.9036	31.972483	74.46	21.51
Linear	10^{16}	1.0892	26.041877	86.15	24.44
Uniform	10^{15}	0.9601	33.225387	81.24	25.92
Linear	**10^{15}**	**1.1037**	**31.749028**	**88.7**	**31.08**

5. Conclusion

This research presents a new design for lead-free perovskite solar cells (PSCs) that addresses the toxicity concerns associated with traditional lead-based PSCs and eliminates the need for a hole transport layer (HTL). The proposed structure has undergone extensive simulations, incorporating investigations on suitable electron transport materials (ETMs), optimization of the electron transport layer (ETL) thickness and doping concentration, optimization of the absorber layer thickness and doping concentration, and analysis of the impact of different doping concentrations on perovskite layer performance. The major advantage of this new design lies in its toxic-free nature and elimination of the HTL, resulting in reduced production costs and complexity, while still maintaining a high level of efficiency. The following conclusions have been derived from the study:

- Proposal of a lead-free perovskite solar cell (PSC) design.
- Elimination of toxicity concerns associated with lead-based PSCs.
- Removal of the hole transport layer (HTL) requirement.
- Extensive simulations and optimization of various structural elements.
- Calibration of simulation results using experimental data.
- Achievement of an efficiency of up to 31.08%.
- Lower production costs and complexity due to toxic-free and HTL elimination.

Reference

[1] Ilke Celik, Adam B. Phillips, Zhaoning Song, Yanfa Yan, Randy J. Ellingson, Michael J. Heben and Defne Apul, Environmental analysis of perovskites and other relevant solar cell technologies in a tandem configuration, Energy & Environmental Science, volume (10), no. 9, pp. 1874–1884, 2017.

[2] Malek Kamal Hussien Rabaia, Mohammad Ali Abdelkareem, Enas Taha Sayed, Khaled Elsaid,Kyu-Jung Chae, Tabbi Wilberforce, A.G. Olabi, Environmental impacts of solar energy systems: A review, Science of the Total Environment, volume (754), 141989, 2021.

[3] Andrew Blakers, Ngwe Zin, Keith R. McIntosh, Kean Fong, High Efficiency Silicon Solar Cells, Energy Procedia, volume (33), Pages 1-10,2013.

[4] Moshsin Ijaz, Aleena Shoukat, Asma Ayub, Huma Tabassum, Hira Naseer, Rabia Tanveer, Atif Islam & Tahir Iqbal, Perovskite solar cells: importance, challenges, and plasmonic enhancement, International Journal of Green Energy, volume (17), pp. 1022-1035,2020.

[5] Bhattarai, S., Kalita, P. K., Hossain, I., Alsubaie, A. S., Mahmoud, K. H., Ansari, M. Z., & Janicek, Designing an Efficient Lead-Free Perovskite Solar Cell through a Computational Method. Crystals, volume (13), no. 8, pp. 1175, July. 2023.

[6] A. Kojima, K. Teshima, Y. Shirai, and T. Miyasaka, Organometal Halide Perovskites as Visible-Light Sensitizers for Photovoltaic Cells, Journal of the American Chemical Society, volume (131), no. 17, pp. 6050–6051, May 2009

[7] Zhiyong Liu, Pengfei Liu, Meng Li, Tingwei He, Tianxiao Liu, Leiming Yu, Mingjian Yuan, Efficient and Stable FA-Rich Perovskite Photovoltaics: From Material Properties to Device Optimization, Advanced Energy Materials, volume (12), no. 18, p. 2200111, Mar. 2022.

[8] Priyanka Roy, Aritra Ghosh, Fraser Barclay, Ayush Khare and Erdem Cuce, Perovskite Solar Cells: A Review of the Recent Advances, Coatings, volume (12), no. 8, p. 1089, Jul. 2022.

[9] Ola Mostafa, Nehad A. Zidan, Wael Abbas, Hanady Hussein Issa, Nihal Gamal, Mostafa Fedawy, Design and Performance Optimization of Lead-Free Perovskite Solar Cells with Enhanced Efficiency, Mathematical Modelling of Engineering Problems, volume (10), no. 4, pp. 1307-1316, August 2023.

[10] Nihal Gamal, Salma H. Sedky, Ahmed Shaker, Mostafa Fedawy, Design of lead-free perovskite solar cell using Zn1-Mg O as ETL: SCAPS device simulation, Optik, volume (242), p. 167306, Sep. 2021.

[11] Mushtaq, S., Tahir, S., Ashfaq, A., Sebastian Bonilla, R., Haneef, M., Saeed, R., Ahmad, W. and Amin, Performance optimization of lead-free MASnBr3 based

perovskite solar cells by SCAPS-1D device simulation. Solar Energy, volume (249), pp.401–413, Jan. 2023.

[12] Fei Zhang and Kai Zhu, Additive Engineering for Efficient and Stable Perovskite Solar Cells, Advanced Energy Materials, volume (10), no. 13, p. 1902579, Oct. 2019.

[13] Feng Hao, Constantinos C. Stoumpos, Duyen Hanh Cao, Robert P. H. Chang & Mercouri G. Kanatzidis, Lead-free solid-state organic–inorganic halide perovskite solar cells, Nature Photonics, volume (8), no. 6, pp. 489–494, May 2014.

[14] M. Burgelman, P. Nollet and S. Degrave, Modelling Polycrystalline Semiconductor Solar Cells, Thin Solid Films, Vol. 361-362, 2000, pp. 527-532, Jul. 10, 2023.

[15] Hui-Jing Du, Wei-Chao Wang and Jian-Zhuo Zhu, Device simulation of lead-free CH 3 NH 3 SnI 3 perovskite solar cells with high efficiency, Chinese Physics B, volume (25), no. 10, p. 108802, Sep. 2016.

[16] Yong Zhang, Xiaotian Hu, Lie Chen, Zengqi Huang, Qingxia Fu, Yawen Liu, Lin Zhang, Yiwang Chen, Flexible, hole transporting layer-free and stable CH3NH3PbI3/PC61BM planar heterojunction perovskite solar cells, Organic Electronics, volume (30), pp. 281–288, Mar. 2016.

[17] K. Bhavsar, P.B. Lapsiwala, Numerical simulation of perovskite solar cell with different material as electron transport layer using SCAPS-1D software, Semiconductor Physics, Quantum Electronics & Optoelectronics, volume (24), No 3. P. 341-347, 2021.

[18] Saif Ahmed, Farihatun Jannat, Md. Abdul Kaium Khan, Mohammad Abdul Alim, Numerical development of eco-friendly Cs2TiBr6 based perovskite solar cell with all-inorganic charge transport materials via SCAPS-1D, Optik, volume (225), p. 165765, Jan. 2021.

[19] Neelima Singh, Alpana Agarwal, Mohit Agarwal, Performance evaluation of lead–free double-perovskite solar cell, Optical Materials, volume (114), p. 110964, Apr. 2021.

[20] Nitin Rai, Shambhavi Rai, Pravin Kumar Singh, Pooja Lohia, D. K. Dwivedi, Analysis of various ETL materials for an efficient perovskite solar cell by numerical simulation, Journal of Materials Science: Materials in Electronics, vol. 31, no. 19, pp. 16269–16280, Aug. 2020.

[21] Atanu Bag , R. Radhakrishnan , Reza Nekovei , R. Jeyakumar, Effect of absorber layer, hole transport layer thicknesses, and its doping density on the performance of perovskite solar cells by device simulation, Solar Energy, volume (196), pp. 177–182, Jan. 2020.